

The effect of cooling rate in thermally sprayed alumina

André Zimmer*

Laboratorio de Materiais Ceramicos, Universidade Federal do Rio Grande do Sul, Av. Osvaldo Aranha, 99/705C-Porto Alegre, RS, Brasil

Particles deposited with a thermal spray process have a large cooling rate during coating formation. In this study, the effect of different cooling rates on plasma sprayed alumina was investigated. The cooling rate of particles has an important effect on alumina phase formation and crystallite size. Basically the corundum phase was observed when cooling rate is low, but with an increase in the cooling rate, nanocrystallites of gamma alumina and amorphous alumina are formed.

Key words: corundum, gamma alumina, amorphous alumina, thermal spray, cooling rate.

Introduction

Thermal spraying is a family of coating processes in which particles, heated and accelerated enough, are deposited onto a substrate. It is well established and represents a technology that is widely used.

Aluminum oxide (alumina, Al_2O_3) is a cheap raw material that has many applications. Due to its high melting point, very high hardness, good chemical stability and low electrical conductivity, it is used in refractories, anti-wear coatings, electronic components, among others.

Liquid alumina solidification is accompanied by a significant volume change. Liquid alumina at its melting point has density of about 2.8 g/cm^3 [1].

As reviewed by Levin and Brandon [2], alumina exists in many metastable polymorphs besides the thermodynamically stable $\alpha\text{-Al}_2\text{O}_3$ (corundum form). The metastable Al_2O_3 structures can be divided into two broad categories: a face-centered cubic (fcc) and a hexagonal close-packed (hcp) arrangement of oxygen anions. The Al_2O_3 structures based on fcc packing of oxygens include γ , η (cubic), θ (monoclinic), and δ (either tetragonal or orthorhombic), whereas the Al_2O_3 structures based on hcp packing are represented by the α (trigonal), κ (orthorhombic), and χ (hexagonal) phases. Some additional Al_2O_3 phases have also been identified.

Corundum, $\alpha\text{-Al}_2\text{O}_3$, is the thermodynamically stable phase of coarsely crystalline aluminum oxide, but syntheses of nanocrystalline Al_2O_3 usually result in $\gamma\text{-Al}_2\text{O}_3$ (gamma alumina). Adsorption microcalorimetry, thermogravimetric analyses, and Brunauer-Emmett-Teller adsorption experiments, coupled with high temperature solution calorimetry data, prove that $\gamma\text{-Al}_2\text{O}_3$ has a lower surface energy than

$\alpha\text{-Al}_2\text{O}_3$ and becomes energetically stable at surface areas greater than 125 square metres per gram and thermodynamically stable at even smaller surface areas (for example, 75 square metres per gram at 800 Kelvin) [3].

An investigation by McHale *et al.* [4] suggests that coarse grained $\gamma\text{-Al}_2\text{O}_3$ should be $+13.4 \pm 2.0 \text{ kJ/mol}$ less energetically stable than $\alpha\text{-Al}_2\text{O}_3$.

Ansell *et al.* [5] results show that melting of $\alpha\text{-Al}_2\text{O}_3$ is accompanied by major structural rearrangements and a change in the Al coordination from octahedral to tetrahedral. Liquid Al_2O_3 exhibits $\gamma\text{-Al}_2\text{O}_3$ like coordination, which leads to the possibility of the formation of $\gamma\text{-Al}_2\text{O}_3$ prior to the formation of the stable $\alpha\text{-Al}_2\text{O}_3$ during rapid solidification. The octahedral aluminum sites found in crystalline $\alpha\text{-Al}_2\text{O}_3$ occur only at the 2% level in liquid alumina [6].

The $\gamma\text{-Al}_2\text{O}_3$ phase has a lower density than the $\alpha\text{-Al}_2\text{O}_3$ phase ($\gamma\text{-Al}_2\text{O}_3$ and $\alpha\text{-Al}_2\text{O}_3$, at room temperature have densities of about 3.66 and 3.99 g/cm^3 , respectively), resulting in the highest volume contraction for $\alpha\text{-Al}_2\text{O}_3$ upon solidification.

Levi *et al.* [7] models predicting the thermal history of alumina powders electrohydrodynamically atomized gave the following results: at approaching 10^5 K/s , there is amorphous phase formation; at somewhat lower cooling rates, the metastable $\gamma\text{-Al}_2\text{O}_3$ can be formed directly from the melt and; at cooling rates in the range of $1\text{-}100 \text{ K/s}$, only $\alpha\text{-Al}_2\text{O}_3$ forms.

The surface where an alumina phase will grow is important too. The study by Ashenford *et al.* [8] shows that $\alpha\text{-Al}_2\text{O}_3$ can grow on the template of a single crystal r-plane sapphire substrate but not on steel substrates. Sapphire possesses the same corundum type structure.

Stahr *et al.* [9] studied the stabilization of alumina using different thermal spray processes and Cr_2O_3 additions in the alumina feedstock. They conclude that there are a large number of open questions regarding the behavior of Al_2O_3 in thermal spray processes and the possibility of stabilizing

*Corresponding author:
Tel : +55 51 3316 3594
Fax: +55 51 3316 3405
E-mail: zimmer@ufrgs.br

the thermodynamically stable corundum still exists.

In this contribution the formation of phases in alumina thermally sprayed at different cooling rates is reported. The resultant crystallite size in the alumina coating will also be discussed.

Experimental

Fused and crushed alumina powder presenting a blocky shape and a mean spherical equivalent diameter of 19 μm (Laser particle size analyzer - Cilas 1180), as showed in Fig. 1, was sprayed by an atmospheric plasma spray with a SG-100 gun onto a rough 304 stainless steel substrate and into a water bath, both at room temperature.

The plasma was operated at 29.3 kW, with argon as the primary and carrier gas and helium as a secondary gas. Flow rates of 56.6, 18.9 and 10 standard litres per minute of respectively primary, secondary and carrier gas. The spray gun stand off distance was 100 mm for deposition on the substrate and 300 mm to collect particles in the water bath.

Scanning electron microscopy (SEM) analysis was used to investigate the coating topography and, morphologies of feedstock and particles captured in water. These materials were sputter coated with about 20 nm film of gold in a Blazers Union SCD 040 sputter-coating machine and then were observed in the scanning electron microscope (Jeol-JSM 6060).

Crystalline phases present in the coating were investigated by X-ray diffraction (XRD) analysis, using an X-ray tube equipped with a Cu target, and operated at an acceleration voltage of 40 kV and a current of 40 mA (Phillips X-ray diffractometer model X'pert MPD).

The XRD analysis was made by the powder method. The coating (detached), the feedstock and the captured particles were milled with a mortar and pestle. A milling technique was used for the coating XRD analysis because of a disprovable size down of nanocrystallites (which is a daunting task) and the stress present in the coating needs to be removed to avoid interference in crystallite size analysis.

From the XRD results, the crystallite size was calculated

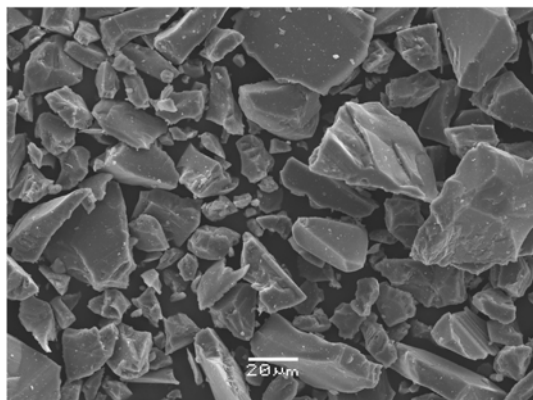


Fig. 1. SEM image of the feedstock.

by the single-line method with Winfit! 1.2 Software [10]. Silicon was used as a standard for instrumental broadening correction.

Results

After the alumina particles pass through the plasma chamber some of them maintained the blocky shape shown in Fig. 1, some acquire round edges or a spherical shape is found as demonstrated in Fig. 2. These transformations could mean that the particles did not melt, partially melted or fully melted.

A top view of a coating in Fig. 3 shows partially and fully spread lamellas. For the particles not soft enough to spread during deposition, it is believed that most of these particles are rebounded, which could explain the observation of no unmelted particles on top of the coating by the SEM observation. Fig. 3 shows two zones of not spread material.

The cracks present in the lamellas of Fig. 3 are a mixture of a complex stress released principally because the cooling process: differential shrinkage between the coating and substrate and a differential volume reduction from the three distinct coating phases - $\gamma\text{-Al}_2\text{O}_3$, amorphous Al_2O_3 and $\alpha\text{-Al}_2\text{O}_3$.

As can be observed in Fig. 4, the phases present in the coating and in the feedstock captured in water are

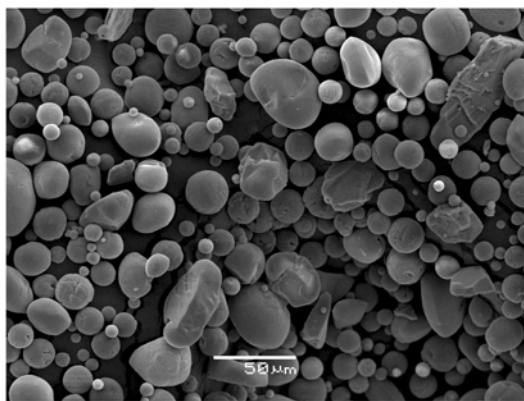


Fig. 2. SEM image from alumina particles collected in water.

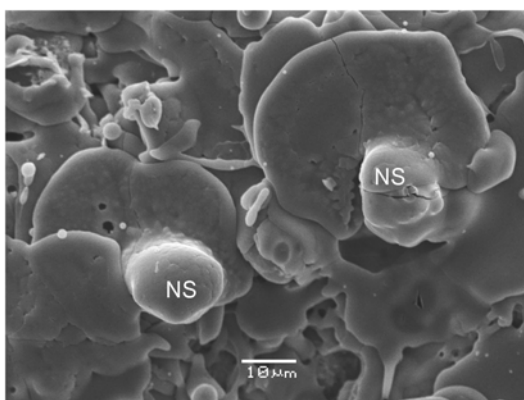


Fig. 3. SEM image from the top of a coating. NS: not spread.

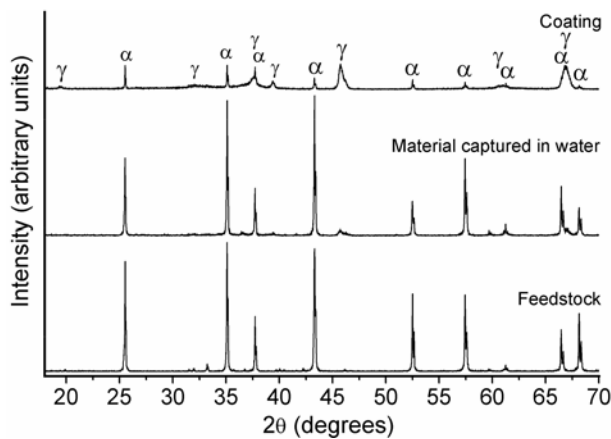


Fig. 4. XRD patterns of the alumina feedstock, of the particles collected in water and of the coating. α : corundum and γ : gamma alumina.

quite different. The coating presents predominantly γ - Al_2O_3 and amorphous alumina, while the particles captured in water is practically all α - Al_2O_3 . The broad hump in the coating diffraction between 20 and 50 degrees of 2θ is a common indication of the presence of the amorphous phase. Gualtieri *et al.* [11] found for a plasma sprayed alumina coating about 84 wt% of γ - Al_2O_3 , 12 wt% of amorphous alumina and 3.7 wt% of α - Al_2O_3 .

Under real quenching conditions in liquid water, the particle is assumed to be in contact both with the liquid and the boiled water. Then, the values of the heat transfer coefficient during a higher stand off distance and in water could be low enough to lead to melted material with cooling rates in the range of where only α - Al_2O_3 forms.

Amorphous alumina could be formed during higher cooling rates at the front area of the deposition. When a particle starts its deposition against the substrate, at the start it experiences a very high heat transfer, which could lead to the presence of the amorphous phase, but during the deposition, somewhat lower cooling rates occurs because of the presence of the γ - Al_2O_3 . Li *et al.* [12] with a high velocity oxy-fuel thermal spray process conclude that high velocity splat quenching of alumina on smooth aluminum, steel and silicon substrates results in suppression of crystallization yielding a predominantly amorphous splat.

If the cooling rate determines the grain width, the front area of the deposition has the highest cooling rates and the lowest grains width. Confirming this, Chraska and King [13] found with transmission electron microscopy, for a plasma sprayed zirconia splat, columnar grains with a width near the substrate ranging from 30 to 70 nm and a grain width in the middle of the splat ranging from 40 to 110 nm and near the top of the splat from 50 to 150 nm.

Then, the zones of not spread material above the splats observed in Fig. 2 could help to form some α - Al_2O_3 or more helpful in forming γ - Al_2O_3 than the formation of the amorphous phase.

The single-line analysis from the XRD analysis of the

coating reveals a medium crystallite size of 18 nm for γ - Al_2O_3 . The α - Al_2O_3 gave crystallite size of about 116 nm. These results are not very precise, because the single-line analysis gives good results in the crystallite size range of 50 and 100 nm. But the broadening in the XRD peaks indicates small crystallite sizes and γ - Al_2O_3 gives peaks which are broader, so it has a smaller crystallite size than α - Al_2O_3 .

In the coating, the presence of the amorphous phase and the small crystallite sizes confirm that the cooling rate could have very high values. Both the presence of amorphous phase and γ - Al_2O_3 phase confirm inhomogeneous cooling rate during deposition.

The cooling rate of the particles during thermal spray deposition is affected by heat transfer of particles that depends on their temperature and heat drainage to the substrate. With an increase of the spraying power there is an increase in the temperature of the particles and this is expected to lead to a decrease in the presence of α - Al_2O_3 in the coating.

To increase the α - Al_2O_3 content in a thermal spray coating for a specific substrate it is necessary to reduce the spraying power deposition, which according to Zhang *et al.* [14], decreases the efficiencies, increases porosity and could reduce residual stresses.

Conclusions

The plasma sprayed particles could melt, be partially melted or fully melted as observed by the captured particles.

The cooling rate of the particles plays an important role in alumina phase formation. Basically α - Al_2O_3 is observed when the cooling rate is low and when the cooling rate is high, both amorphous and γ - Al_2O_3 are found.

In the coating, γ - Al_2O_3 appears with a nanometric crystallite size, while α - Al_2O_3 could be considered present with a micrometric crystallite size.

It seems to be difficult to increase the presence of α - Al_2O_3 to a majority phase in a coating which is thermally sprayed:

- First, for a fully melted particle, it is necessary during high cooling rates to have an important rearrangement in the Al_2O_3 structure from liquid to the α - Al_2O_3 arrangement.
- Second, high cooling rates lead to solidification with lower crystal sizes and in this situation, the surface energy is more favorable for the formation of γ - Al_2O_3 than for α - Al_2O_3 .
- Third, an increase in not fully melted particles or lower cooling rates could lead to an increase of the presence of α - Al_2O_3 , costing both an increase of crystallite sizes and not well spread particles and, the latter could lead to a lower densification.

Acknowledgements

The Brazilian Federal Research Agency CNPq is acknowledged for the financial support and Elfusa Company is acknowledged for the donation of electrofused alumina.

References

1. B. Glorieux, F. Millot, J.-C. Rifflet and J.-P. Coutures, *Int. J. Thermophys.* 20[4] (1999) 1085-1094.
2. I. Levin and D. Brandon, *J. Am. Ceram. Soc.* 81[8] (1998) 1995-2012.
3. J.M. McHale, A. Auroux, A.J. Perrotta and A. Navrotsky, *Science*. 277[788] (1997) 788-791.
4. J.M. McHale, A. Navrotsky and A.J. Perrotta, *J. Phys. Chem. B.* 101[4] (1997) 603-613.
5. S. Ansell, S. Krishnan, J.K.R. Weber, J.J. Felten, P.C. Nordine, M.A. Beno, D.L. Price and M.-L. Saboungi, *Phys. Rev. Lett.* 78[3] (1997) 464-466.
6. C. Landron, L. Hennet, T.E. Jenkins, G.N. Greaves, J.P. Coutures and A.K. Soper, *Phys. Rev. Lett.* 86[21] (2001) 4839-4842.
7. C.G. Levi, V. Jayaram, J.J. Valencia and R. Mehrabian, *J. Mater. Res.* 3[5] (1988) 969-983.
8. D.E. Ashenford, F. Long, W.E. Hagston, B. Lunn and A. Matthews, *Surf. Coat. Tech.* 116-119 (1999) 699-704.
9. C.C. Stahr, S. Saaro, L.-M. Berger, J. Dubsky, K. Neufuss and M. Herrmann, *J. Therm. Spray Techn.* 16[5-6] (2007) 822.
10. S. Krumm, *Mat. Sci. Forum.* 228-231[PART 1] (1999) 183-188.
11. M.L. Gualtieri, M. Prudenziatia and A.F. Gualtieri, *Surf. Coat. Tech.* 201[6] (2006) 2984-2989.
12. L. Li, B. Kharas, H. Zhang and S. Sampath, *Mat. Sci. Eng. A-Struct.* 456[1-2] (2007) 35-42.
13. T. Chraska and A.H. King, *J. Mater. Sci. Lett.* 18[18] (1999) 1517-1519.
14. J. Zhang, H. Chen, T. Sekino, S.H. Kim and S.W. Lee, *J. Ceram. Proc. Res.* 9[3] (2008) 317-320.